

Available online at [www.sciencedirect.com](http://www.sciencedirect.com)**ScienceDirect**

Nuclear Physics A 982 (2019) 855–858

[www.elsevier.com/locate/nuclphysa](http://www.elsevier.com/locate/nuclphysa)

# Hidden strangeness shines in NA61/SHINE

Antoni Marcinek for the NA61/SHINE Collaboration

*Institute of Nuclear Physics, Polish Academy of Sciences, Kraków, Poland*

## Abstract

Preliminary results on the  $\phi$  (1020) meson production in inelastic proton-proton collisions measured by the NA61/SHINE experiment at the CERN SPS are presented in these proceedings. The results include the first ever differential  $p_T$  and  $y$  measurements at beam momenta of 40 and 80 GeV and the most ever detailed experimental data at 158 GeV. The comparison of  $p + p$  to Pb + Pb results shows a non-trivial system size dependence of the widths of the rapidity distributions for  $\phi$  mesons, contrasting with that of other hadrons. The results are furthermore compared to the world data on  $\phi$  meson production, demonstrating the better accuracy achieved by the NA61/SHINE experiment, and to several models. None of the models is found to be able to describe simultaneously the shape of transverse momentum spectra, the shape of rapidity distribution and the total yield.

**Keywords:**  $\phi$  (1020) production, CERN, SPS

## 1. Introduction

Motivation for the measurement of hidden strangeness —  $\phi$  (1020) meson consisting of  $s$  and  $\bar{s}$  valence quarks — in  $p + p$  collisions at CERN SPS energies is twofold. On one hand, it may serve to constrain hadron production models, for which the hidden strangeness treatment is particularly interesting. On the other hand, it may be used as reference for Pb + Pb measurements at the same energies to infer strangeness-related phenomena in heavy ion collisions.

The measurement presented here was conducted within the two-dimensional scan, in beam momentum and size of the colliding system, performed by the NA61/SHINE experiment [1] to explore properties of strongly interacting matter. The analysis, described in detail in Ref. [2], is done by means of tag-and-probe invariant mass spectra fits in the  $\phi \rightarrow K^+ K^-$  decay channel. For brevity, the present document uses natural units.

## 2. Differential spectra

Multiplicities of  $\phi$  mesons in  $p + p$  collisions are obtained as a function of the rapidity ( $y$ ) and of transverse momentum ( $p_T$ ) for beam momenta of 158 GeV ( $\sqrt{s_{NN}} = 17.3$  GeV), 80 GeV ( $\sqrt{s_{NN}} = 12.3$  GeV) and 40 GeV ( $\sqrt{s_{NN}} = 8.8$  GeV). These are the first ever differential measurements of  $\phi$  production at 40 and 80 GeV and the first double-differential measurements at 158 GeV.

<https://doi.org/10.1016/j.nuclphysa.2018.10.041>

0375-9474/© 2018 Published by Elsevier B.V.

This is an open access article under the CC BY-NC-ND license (<http://creativecommons.org/licenses/by-nc-nd/4.0/>).

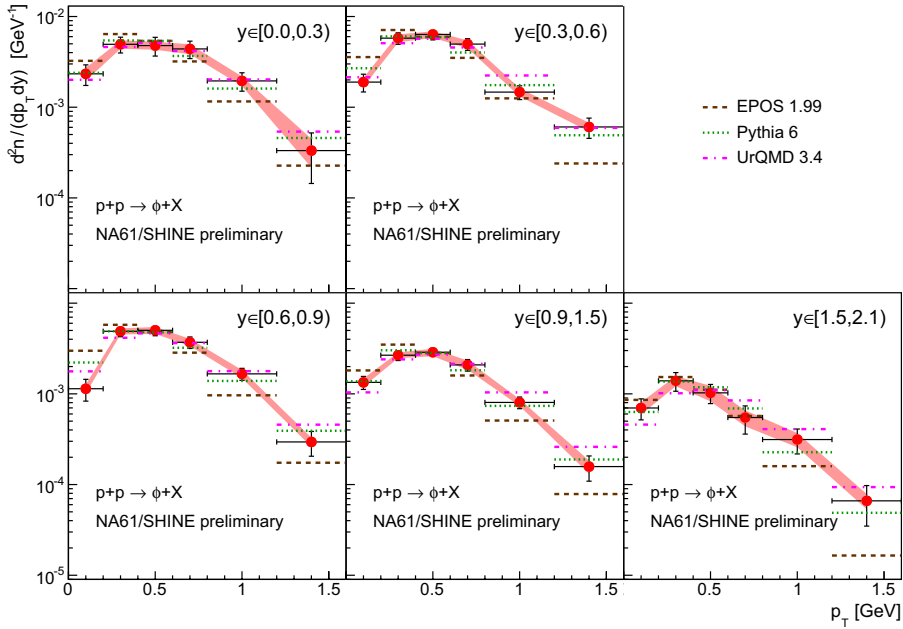


Fig. 1: Transverse momentum spectra of  $\phi$  mesons in  $p + p$  collisions at 158 GeV beam momentum ( $\sqrt{s_{NN}} = 17.3$  GeV) in different rapidity intervals with statistical (vertical lines) and systematic (bands) uncertainties compared to different models (as can be seen in the legend). Horizontal lines give  $p_T$  interval sizes.

In Fig. 1 one can see a comparison of  $p_T$  spectra measured at 158 GeV to three models: Epos 1.99 [3, 4] from the CRMC 1.6.0 package [5], PYTHIA 6.4.28 [6] and URQMD 3.4 [7, 8]. These models are normalized to the integral of the data in each rapidity interval, in order to compare the shapes of  $p_T$  spectra between experimental data and models. One finds that PYTHIA (green dotted line) describes well the  $p_T$  spectra shapes, while the spectra from URQMD (long dashed black line) are too hard and those from EPOS (dashed magenta lines) too soft.

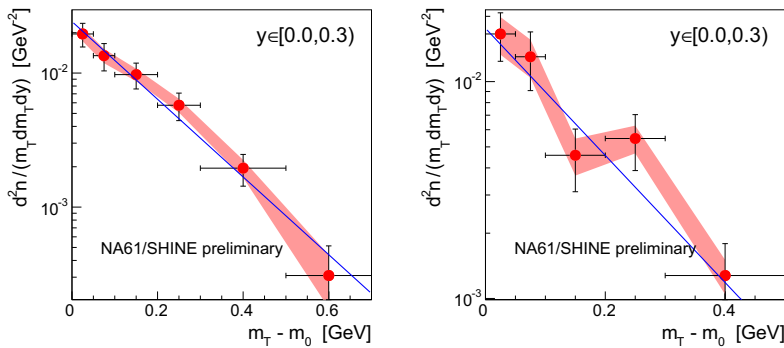


Fig. 2: Transverse mass spectra at midrapidity for  $\phi$  mesons in  $p + p$  collisions at beam momenta of 158 GeV (left,  $\sqrt{s_{NN}} = 17.3$  GeV) and 80 GeV (right,  $\sqrt{s_{NN}} = 12.3$  GeV), with statistical (vertical lines) and systematic (bands) uncertainties. Horizontal lines give  $m_T$  interval sizes. The rest mass ( $m_0$ ) of the  $\phi$  is taken from PDG [9]. The blue lines represent the exponential fit to the data. See the text for details.

In Fig. 2, the transverse mass ( $m_T$ ) spectra obtained at midrapidity for beam momenta of 158 GeV (left panel) and 80 GeV (right panel) are shown. Exponential fits are performed to obtain the inverse slope parameter, which represent the effective temperature ( $T$ ) of the system created after the collision. The temperature parameters obtained from the fit ( $T = (150 \pm 14(\text{stat.}) \pm 8(\text{syst.}))$  MeV for 158 GeV collisions and  $T = (148 \pm 30(\text{stat.}) \pm 17(\text{syst.}))$  MeV for the 80 GeV collisions) are consistent within uncertainties with the temperature parameters determined for charged pions and kaons [10].

### 3. Widths of the rapidity distributions

The  $p_T$ -integrated rapidity distributions are obtained by summing and extrapolating the double differential spectra of  $y$  and  $p_T$  for 80 GeV and 158 GeV collisions. For 40 GeV beam momentum, due to limited statistics, rapidity spectrum is obtained directly as a result of a single differential analysis. Figure 3 shows the width ( $\sigma_y$ ; see Ref. [2] for the details of its estimation for each data set) of the rapidity distributions for the  $\phi$  mesons and for other particles ( $\pi$ ,  $K$ ,  $\Lambda$ ) produced in  $p + p$  (open markers) and central Pb + Pb collisions (full markers) [10–16] as a function of the beam rapidity ( $y_{\text{beam}}$ ) in the centre-of-mass frame. It is clear that that all particles in both colliding systems follow the same trend, *except for the  $\phi$  in Pb + Pb*. This non-trivial system size dependence for  $\phi$  mesons, contrasting with all the other measured hadrons, calls for investigation in other systems measured within the beam momentum and system size scan of NA61/SHINE.

The measured widths have also been compared to those expected from models in the right panel of Fig. 3. PYTHIA (inverted-triangular green markers) produces too narrow  $\phi$  rapidity spectra, while both EPOS (triangular brown markers) and UrQMD (magenta crosses) provide widths comparable to experimental data. Moreover, Fig. 3 demonstrates that the experimental results are not compatible with predictions of the simple  $K^+K^-$  coalescence model [13] (dotted and solid thick black lines).

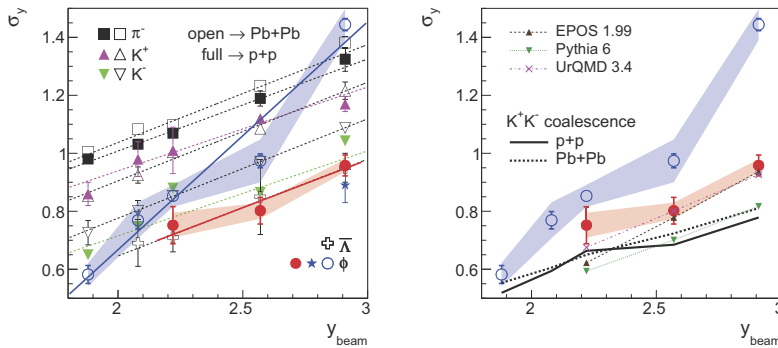


Fig. 3: *Left*: Widths of rapidity distributions ( $\sigma_y$ ) of different particles produced in  $p + p$  (full symbols) and in central Pb + Pb (open symbols) collisions as a function of beam rapidity, with statistical (vertical lines) and systematic (bands) uncertainties. For the  $\phi$  measurement, full red circles are the results reported in this analysis, while the blue star comes from the NA49  $p + p$  measurement [11]. Results for other particles produced in  $p + p$  come from NA61/SHINE [10, 12], while data from Pb + Pb collisions are from NA49 [13–16]. Lines are fitted to points to guide the eye. *Right*: Comparison of the widths of the rapidity distributions of  $\phi$  mesons with expectations from kaon coalescence (black lines) and different models, are reported on the legend.

### 4. Total and midrapidity yields

The energy dependence of the total ( $\langle\phi\rangle$ ) and midrapidity ( $\frac{dn}{dy}(y=0)$ ) yields of the  $\phi$  mesons produced in  $p + p$  interactions are shown in left and right panels of Fig. 4, respectively. It is evident that NA61/SHINE results are consistent with the world data [11, 17–23], but are much more accurate. Comparing to the models, it is possible to observe that while EPOS describes the data reasonably well (although the rise with collision energy is too fast), all the other models fail with UrQMD and PYTHIA significantly underestimating and HRG [24] overestimating the yield by about a factor of 2.

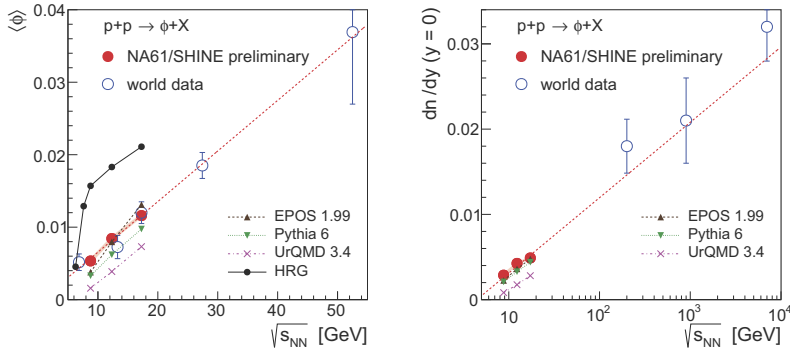


Fig. 4: Energy dependence of the total yields (left panel) and yields evaluated at midrapidity (right panel) of the  $\phi$  mesons produced in  $p + p$  collisions. World data come from Refs. [11, 17–23]. Only total uncertainties are shown on the plot. For preliminary NA61/SHINE results total uncertainties are smaller than markers. Red dashed lines are fitted to guide the eye.

## 5. Summary

Preliminary results on the  $\phi$  (1020) meson production in inelastic proton-proton collisions at beam momenta of 40, 80 and 158 GeV, measured by the NA61/SHINE experiment, were shown. These results are consistent with the world data on  $\phi$  meson production in  $p + p$  collisions, but demonstrate better accuracy achieved by the NA61/SHINE experiment. Comparison with several models shows, that none of these models is able to describe simultaneously the shape of transverse momentum spectra, the shape of rapidity distribution and the total yield. Finally, the comparison of  $p + p$  to Pb + Pb results shows a non-trivial system size dependence of the widths of the rapidity distributions for  $\phi$  mesons, contrasting with that of other hadrons.

This work was supported by the National Science Centre, Poland (grant numbers: 2014/14/E/ST2/00018, 2015/18/M/ST2/00125).

## References

- [1] N. Abgrall, et al., JINST 9 (2014) P06005.
- [2] A. Marcinek, Ph.D. thesis, [https://edms.cern.ch/file/1736151/1/Antoni\\_Marcinek\\_PhD.pdf](https://edms.cern.ch/file/1736151/1/Antoni_Marcinek_PhD.pdf) (2016).
- [3] K. Werner, F. Liu, T. Pierog, Phys. Rev. C 74 (2006) 044902.
- [4] T. Pierog, K. Werner, Nucl. Phys. B (Proc. Suppl.) 196 (2009) 102.
- [5] C. Baus, T. Pierog, R. Ulrich, CRMC (Cosmic Ray Monte Carlo package).
- [6] T. Sjöstrand, S. Mrenna, P. Skands, J. High Energy Phys. 05 (2006) 026.
- [7] S. Bass, et al., Prog. Part. Nucl. Phys. 41 (1998) 255.
- [8] M. Bleicher, et al., J. Phys. G 25 (1999) 1859.
- [9] K. Olive, et al., Chin. Phys. C 38 (2014) 090001.
- [10] A. Aduszkiewicz, et al., Eur. Phys. J. C 77 (2017) 671.
- [11] S. Afanasiev, et al., Phys. Lett. B 491 (2000) 59.
- [12] N. Abgrall, et al., Eur. Phys. J. C 74 (2014) 2794.
- [13] C. Alt, et al., Phys. Rev. C 78 (2008) 044907.
- [14] S. V. Afanasiev, et al., Phys. Rev. C 66 (2002) 054902.
- [15] C. Alt, et al., Phys. Rev. C 77 (2008) 024903.
- [16] T. Anticic, et al., Phys. Rev. Lett. 93 (2004) 022302.
- [17] V. Blobel, et al., Phys. Lett. B 59 (1975) 88.
- [18] C. Daum, et al., Nucl. Phys. B 186 (1981) 205.
- [19] D. Drijard, et al., Z. Phys. C 9 (1981) 293.
- [20] M. Aguilar-Benitez, et al., Z. Phys. C 50 (1991) 405.
- [21] B. I. Abelev, et al., Phys. Rev. C 79 (2009) 064903.
- [22] K. Aamodt, et al., Eur. Phys. J. C 71 (2011) 1594.
- [23] B. Abelev, et al., Eur. Phys. J. C 72 (2012) 2183.
- [24] V. Vovchenko, V. V. Begun, M. I. Gorenstein, Phys. Rev. C 93 (2016) 064906.